Partial Analysis of LDEF Experiment A-0114

Final Report on Contract NAS8-36645

for the reporting period May 20, 1985 - November 19, 1991

Dr. John C. Gregory, Principal Investigator
Department of Chemistry
Materials Science Building, Room 111
The University of Alabama in Huntsville
Huntsville, Alabama 35899

John C. Gregory
NAS8-36645

During the contract period, work has concentrated on four main components. Data from the UAH silver pin hole camera was analyzed for determination of the mean LDEF satellite attitude and stability in orbit, to include pitch and yaw. Chemical testing performed on the AO-114 hot plate determined the form and locus of absorption of cosmogenic beryllium-7. Reaction rates of atomic oxygen with Kapton and other polymeric solids integrated over the whole LDEF orbital lifetime were analyzed. These rates were compared with the JSC estimated values for Space Station exposures. Metal and polymer films exposed on A0114 (C-9 and C-3 plates) were also analyzed. The following papers which report these finding have appeared or have been accepted for publication.

1) "Observation of ^{7}Be on the Surface of LDEF Spacecraft". Fishman, G.J., Harmon, B.A., Gregory, J.C., Parnell, T.A., Peters, P., Phillips, G.W., King, S.E., August, R.A., Ritter, J.C., Cutchin, J.H., Haskins, P.S., McKisson, J.E., Ely, D.W., Weisenberger, A.G., Piercey, R.B., and Dybler, T.: Nature, 349, 1991, pp678-680.

2) "A Measurement of the Attitude Stability of the LDEF Satellite Using a Silver/Silver Oxide Detector", J.C. Gregory, P.N. Peters, Journal of Guidance, Control and Dynamics, AIAA, Vol. 15, No. 1, Jan-Feb, 1992, pp 282-284.

3) "Measurements of Erosion Characteristics for Metal and Polymer Surfaces Using Profilometry", J. C. Gregory, L.C. Christl and P.N. Peters, Proceedings of the LDEF First Post-retrieval Symposium, Orlando, Florida, June, 1991.

4) "Pinhole Cameras as Sensors for Atomic Oxygen in Orbit: Application to Attitude Determination of the LDEF", J.C. Gregory and P.N. Peters, Proceedings of the LDEF First Post-retrieval Symposium, Orlando, Florida, June, 1991.

MEASUREMENTS OF EROSION CHARACTERISTICS FOR METAL AND POLYMER SURFACES USING PROFILOMETRY

Ligia C. Christl and John C. Gregory
The University of Alabama in Huntsville*
Huntsville, Alabama 35899
Phone: 205/895-6840, Fax: 205/895-6349

Palmer N. Peters
Space Science Laboratory, NASA/MSFC
Huntsville, Alabama 35812
Phone: 205/544-7728, Fax: 205/544-7754

SUMMARY

The surfaces of many materials exposed in low earth orbit are modified due to interaction with atomic oxygen. Chemical changes and surface roughening effects can occur which alter optical and other properties (ref.1). The experiment A0114 contained 128 solid surface samples, half of which were exposed on the front and half on the rear of LDEF. Each sample has been subjected to many analyses, but this paper will only describe the methods and techniques used to measure the changes in roughness, erosion depths and material growth using profilometry.

INTRODUCTION

The effect of atomic oxygen on materials is highly variable. No method of measuring the effects is optimum for all materials. We have developed several techniques found valuable in analyzing a wide range of materials, varying from minute effects on the level of atomic dimensions to heavily etched surfaces. One of the most effective techniques has been to utilize the measurement of etched steps at interfaces between exposed and unexposed, or masked, areas by stylus profilometry. Stylus profilometers typically measure the vertical displacement of a stylus (usually a fine pointed diamond) as it is scanned horizontally across the surface. Highly magnified vertical displacements are plotted against horizontal positions greatly exaggerating surface detail. This technique has the ability to measure a wide range of etch steps, from below 1 nm to 1 mm. For measurements below 1 nm it is essential that optically flat surfaces be used and that the steps be measurable over very short lateral distances. As shown elsewhere (ref.2), to produce etch steps over short lateral distances requires very thin masks, preferably thin film patterns resistant to atomic oxygen that are strongly bonded to the substrate being exposed, or at least knife-edged masks essentially in contact with the surface; these types of mask avoid structures which

* Work supported in part by a grant from UAH Research Institute and NASA grant NAGW-812 and contract NAS8-36645.

shadow the sample from the incident oxygen, preventing etch profiles with wide lateral dimensions. Lack of shadowing is particularly important on surfaces experiencing little effect, since even optical flats have variations or waves on their surfaces which cannot be distinguished from etch steps unless the steps are very sharp or patterned. One of the best patterns is a series of closely spaced lines for the masks, which produce a square wave pattern in the surface, providing multiple steps for comparison. An alternative approach for some thin films is to scratch narrow grooves through the thin film but without damaging the substrate. The depth of the scratches in both exposed and unexposed regions is then measured at a number of locations. This works well for materials softer than glass but hard enough to avoid excessive formation of furrows adjacent to the scratches. When done properly, the scribe will not scratch the substrate and will leave a flat bottom in the scratched area, indicating the full thickness of the film has been removed, as opposed to a v-shaped scratch which offers no assurance of this. Not only can etch steps be measured this way, but contaminant layers or increases in thicknesses in exposed areas due to oxidation or other causes, can be determined accurately, sometimes to a few 0.1 nm. This latter ability is valuable in conjunction with optical measurements on thin films where it is not known whether an increase in light transmission is due to a thinning of pathlength by removal of material or a change in optical properties. Measurement of an increase in the film thickness in the exposed areas helps to establish the latter. Thus, some metals have volatile oxides and are thinned while some form stable, clear oxides and are thickened, but are more transmissive to light. Good reflectance measurements are also desired in conjunction with the transmission measurements to account for any contamination or surface changes.

MEASUREMENTS

A wide variety of material surfaces were exposed to the atomic oxygen fluence, UV degradation and space contamination in the LDEF-A0114 experiment. The atomic fluence for the LDEF was 9.73×10^{21} atom cm^{-2} over its nearly six years exposure.

The surfaces consisted of polished bulk samples and high purity thin optical metal films sputtered or evaporated onto 1 inch flat fused silica disks. Each disk had one half of its surface masked, to be used as a control surface, and the other half was exposed to the environment. The samples were mounted in an aluminium panel, as shown in Figure 1. By masking half of each sample, it was possible to measure changes in roughness, erosion depths, material growth and changes in film thickness. These changes were measured, using a Taylor-Hobson Talystep Profilometer, model number 223-27, and a Taylor-Hobson Form Talysurf, model number 279-17.

The Talystep is a surface-profiling instrument designed to measure micro-thin film deposits, with a height resolution of ~1 Å and a lateral resolution of ~1μ. The one used for our measurements consisted of a conical diamond tip stylus of 1μm radius, with an adjustable force of 1 to 30 mgf. One mgf was used for tracing soft metals like Au, Ag and Sn films, to minimize damage to the surface. The Talystep measures the thickness of a film by moving the stylus at a constant rate across a groove cut in the film or across the step between the film and the substrate at the edge of the sample. To minimize thermal gradients and vibrations that affect the performance of the instrument on the most sensitive scales, the Talystep is enclosed in a plexiglas box and mounted on a vibration isolation table that in turn is placed on a granite slab in an air conditioned room (ref.3)

Calibration of the instrument was done using a standard provided by Taylor-Hobson. It is comprised of a frame and a base on which two glass plates are mounted. For checking the lower magnification ranges the left hand plate has three grooves nominally 2.5 micrometer deep with an

uncertainty of ± 0.05 μm. To check the highest magnification; the right-hand plate has three grooves nominally 0.025 μm deep with an uncertainty of ± 0.005 μm.

The Talysurf instrument is similar to the Talystep but operates over larger ranges with lower resolution. The program supplied with this instrument is able to measure many different shapes. Also, the stylus loading force is much greater, with a range from 75 to 100 mgf. A statistical analysis package, provided with the system, calculates both the mean value and standard deviation of the data values obtained from a series of measurement. Corrections for the accurate movement of the stylus arm and the size and shape of stylus tip are made by the computer. In order for the computer to make these corrections, a series of constants, whose values represent the characteristics of the individual stylus geometry, are required. These constants can be input via the keyboard or determined from a calibration routine automatically.

DISCUSSION

Examples of applications of stylus profilometry to different materials illustrate its ability to measure numerous features of exposed and unexposed surfaces. Nine examples will be discussed here. Figure 2 illustrates the ability to measure the roughness of a typical coated surface (unexposed iridium) on an optical flat of moderate quality. The RMS roughness is strongly influenced here by the longer period wave on the surface compared to the short period roughness. A sharp transition is shown in Figure 3 for an iridium sample scanned from exposed to unexposed areas. Even though the surface has a wave associated with it, a step of ~3.6 nm increase in thickness on the exposed area is apparent. The roughness on the exposed surface is also obviously increased by spikes which so far have not been satisfactorily explained. The increase in thickness could result from contamination or modification of the film itself. Studies are still underway to interpret the cause. Figure 4 represents a stylus trace on the same iridium sample from unexposed to exposed area. Although the roughness of the exposed area varies over the surface, the increase in thickness is comparable (3.5 nm and 3.6 nm), except at the knife edge boundary for Figure 4; although the sloped surface of the knife edge might enhance contamination effects at the boundary, insufficient data exists to positively identify the cause of the feature.

The gold film also shows a similar increase in thickness on the exposed area (~3.5 nm) however the gold surface does not exhibit the spikes on the exposed surface that were observed on the iridium surface. Figure 5 shows a stylus trace across one scratch in the unexposed area. Figure 6 shows a stylus trace across two scratches in the exposed region. Note that the rms roughness includes the depth of the scratches. The actual rms roughness on exposed was ~1.0 nm and the unexposed was ~ 0.7 nm for the gold sample.

Figure 7 shows how multilayer coatings can be resolved by the scratching and profiling, in some cases. In this figure a silver film deposited over a carbon film was investigated. The two scratches gave ~19.4 nm and ~20.1 nm for the unexposed carbon thickness and ~33.3 and ~31.3 nm for the unexposed silver thickness. The exposed portion of the silver over carbon sample could not be resolved into two layers, but only one. The total thickness of this exposed area averaged ~112.2 nm compared to the total of ~52 nm for the unexposed area. See Figure 8.

Figure 9 illustrates etching of polycrystalline carbon of such magnitude that the etch depth exceeds the range of the Talystep used above and required the use of the Talysurf. The very rough nature of exposed combustible materials that erode heavily with formation of volatile products has been documented by SEM and other imaging techniques. The stylus profilometer provides

accurate measurements of the spikes or plateaus that form at locations of slower etch, and provides an estimate of the maximum etch depth.

Polymethylmethacrylate, PMMA, is a plastic which is readily etched by atomic oxygen, forming a large number of small spikes at the bottom of the etch and a large etch step, as shown in Figure 10, and Figure 11. Figure 10, was traced on a sample mounted on the ambient temperature plate and Figure 11 is for a sample mounted on a separate thermally isolated plate of semipolished aluminum. The purpose was to examine the etch rate as a function of temperature. The small increase in etch in Figure 11 may be due to slightly higher temperature of the hot plate sample. The smooth plateau at the right of the etched area in Figure 10 is due to an artefact caused by the stylus catching on the large etch step and dragging the sample a short distance; heavily etched samples need to be secured for this reason.

CONCLUSION

Stylus profilometry is a very effective non destructive or minimal scratching technique to measure roughness, erosion depth and material growth of metals, polymers and carbons exposed to the atomic oxygen.

We have demostrated that these instruments (Talystep and Talysurf), used in combination with some of the techniques mentioned (scratching, step and transition measurements), have a wide range of resolutions, from ~1Å to a few hundred microns.

Examples, like iridium film, show the reliability of the instrument, giving the same thickness value for the transition in any direction scanned.

Stylus profilometry, by indicating decreases, or increases, in film thicknesses enables interpretations of changes in optical density measurements, i.e. whether thinning of the film or an increase in thickness with optical property changes are responsible for optical density changes.

REFERENCES

1. Peters, P.N., Gregory, J.C., and Swan, J.T., "Effects on Optical Systems from Interactions with Oxygen Atoms in Low Earth Orbits," Applied Optics, 25, 1290-1298 (1986).

2. Peters, P.N., Sisk, R. C., and Gregory, J.C., "Velocity Distributions of Oxygen Atoms Incident on Spacecraft Surfaces," J. Spacecraft and Rockets, 25(1), 53-58 (1988).

3. Bennett, J. M., and Dancy, J. H., "Stylus Profiling Instrument for Measuring Statistical Properties of Smooth Optical Surfaces," Applied Optics, 20, 1785-1802 (1981).

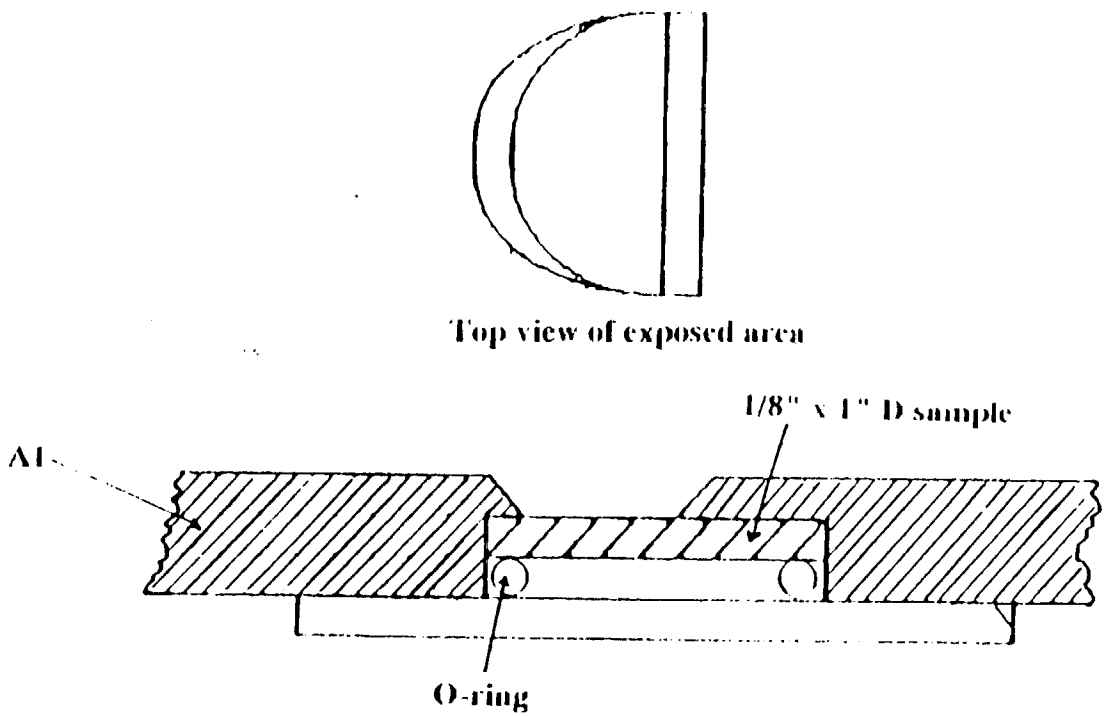

Figure 1. Cross-section of sample holder between exposed and unexposed areas

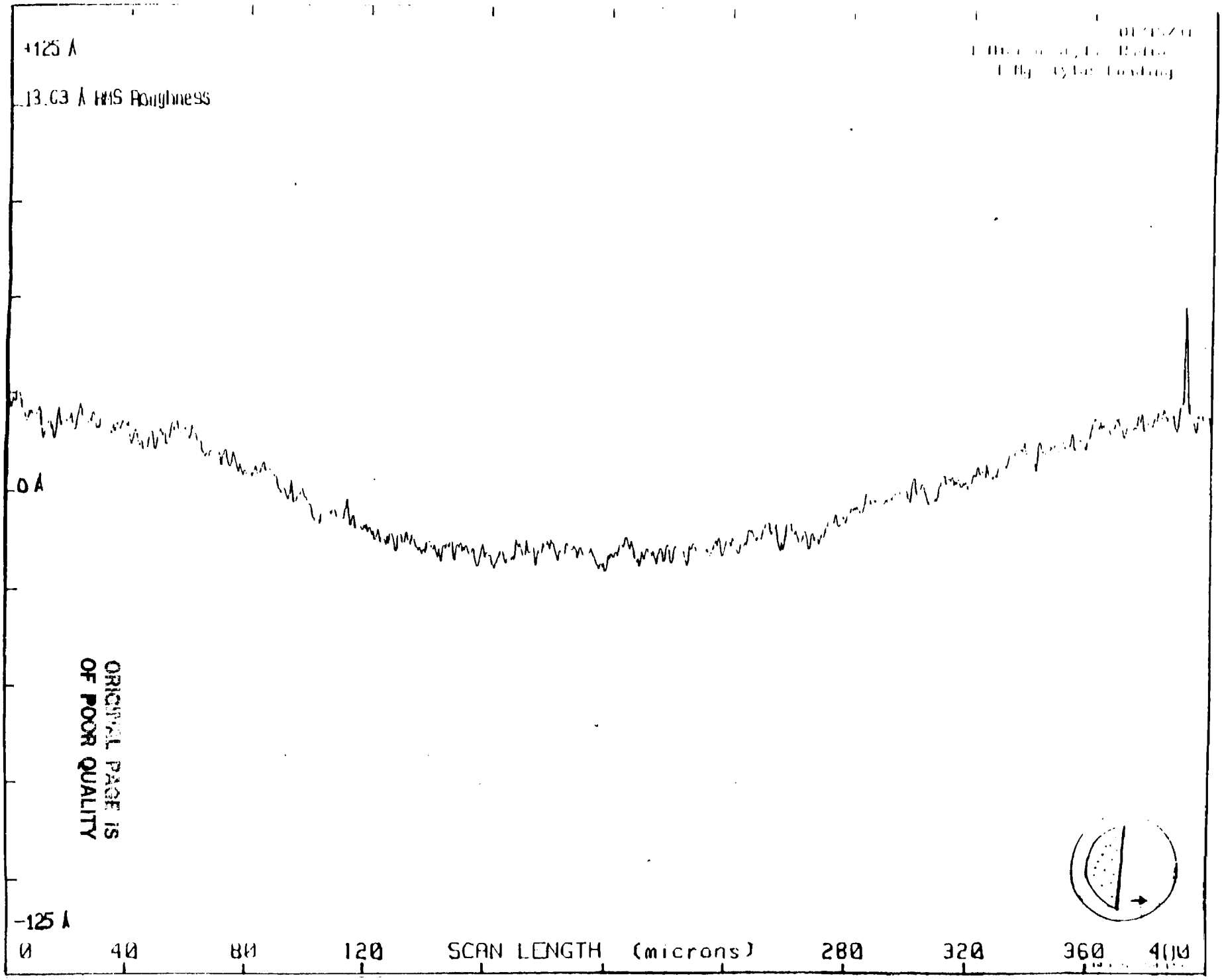

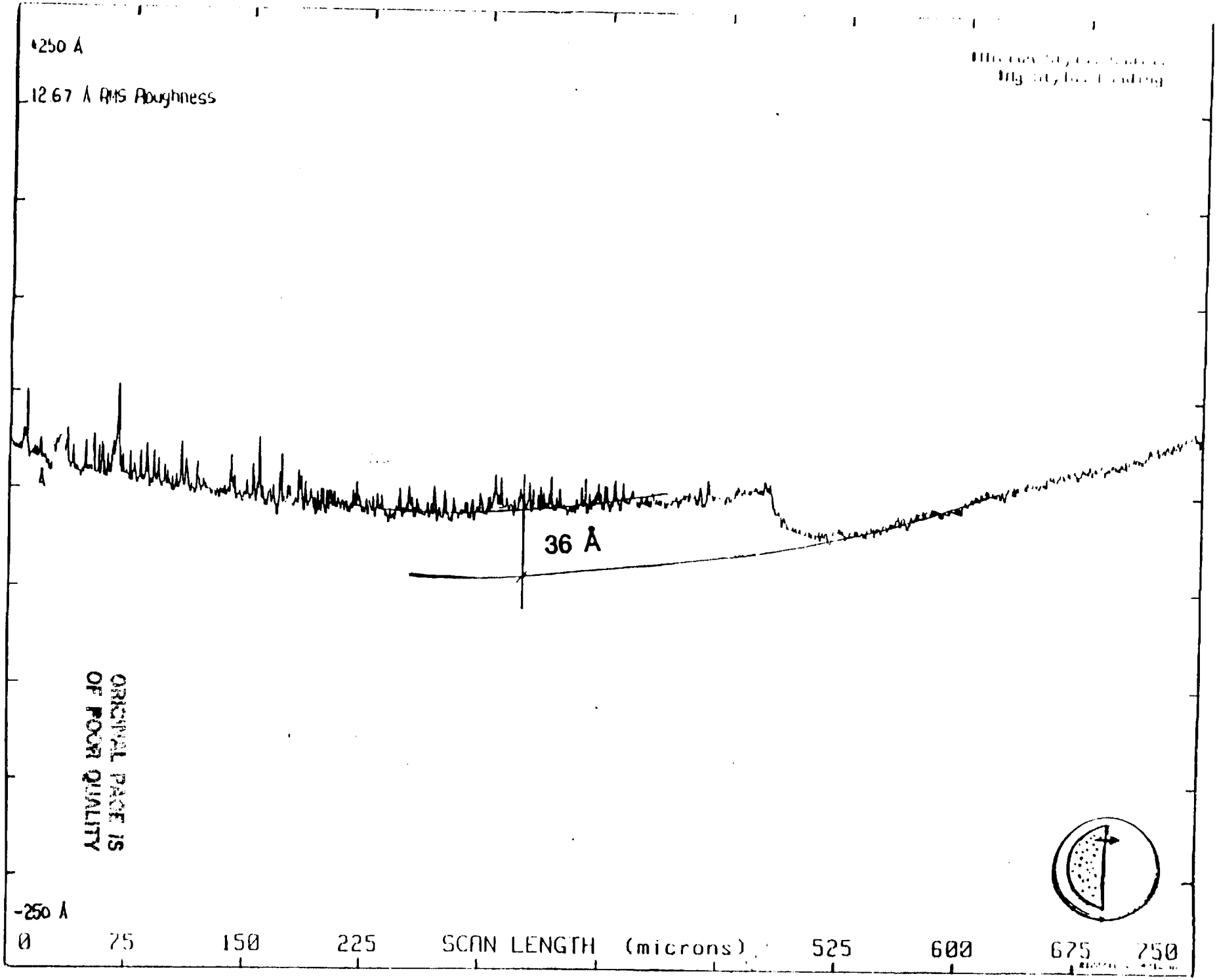
250 Å
12.67 Å RMS Roughness
36 Å
-250 Å
0
75
150
225
SCAN LENGTH (microns)
525
600
675
750
ORIGINAL PAGE IS
OF POOR QUALITY

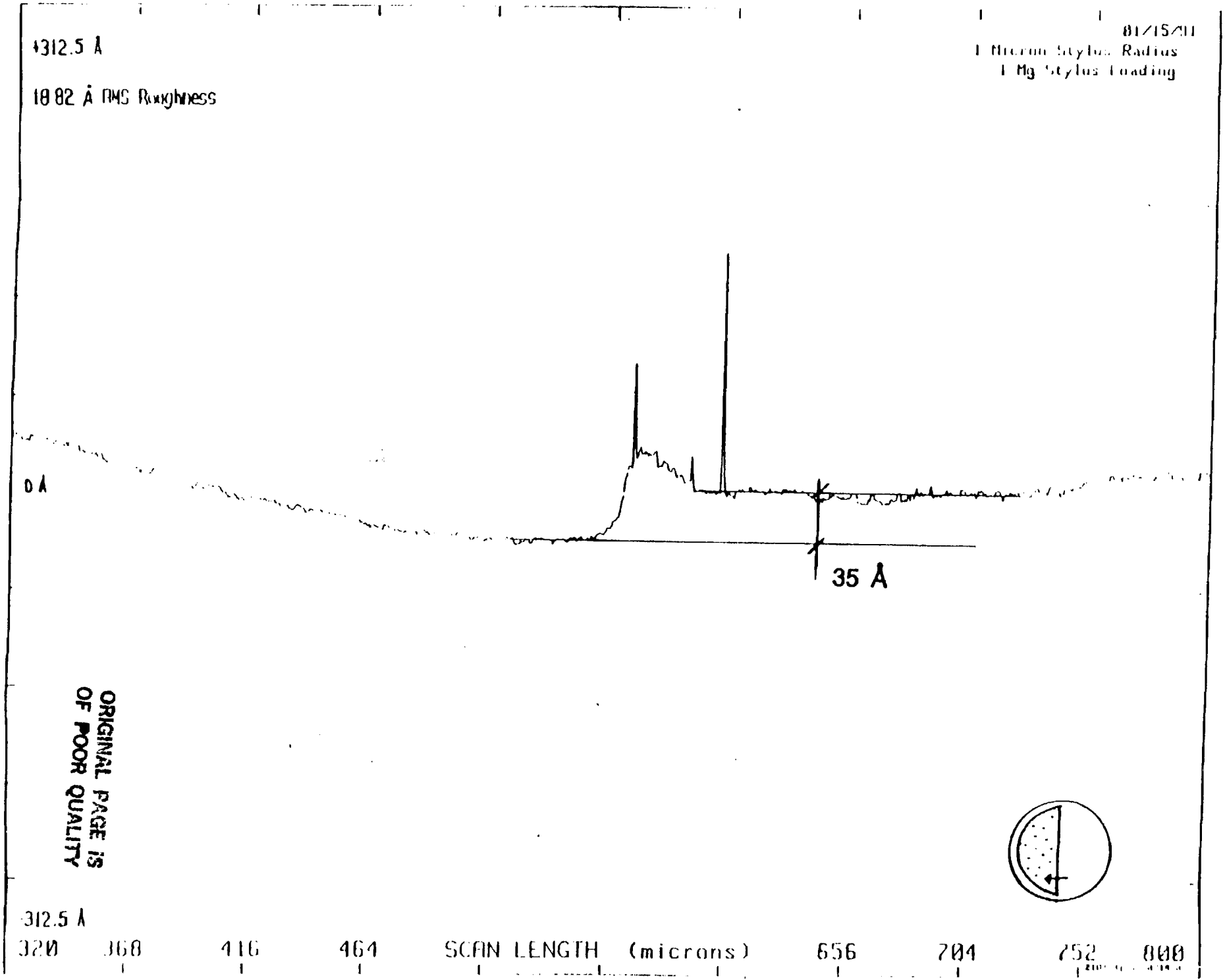
4312.5 Å
1882 Å RMS Roughness
81/15/01
1 Micron Stylus Radius
1 Mg Stylus Loading
0 Å
35 Å
ORIGINAL PAGE IS
OF POOR QUALITY
-312.5 Å
320
368
416
464
SCAN LENGTH (microns)
656
704
752
800

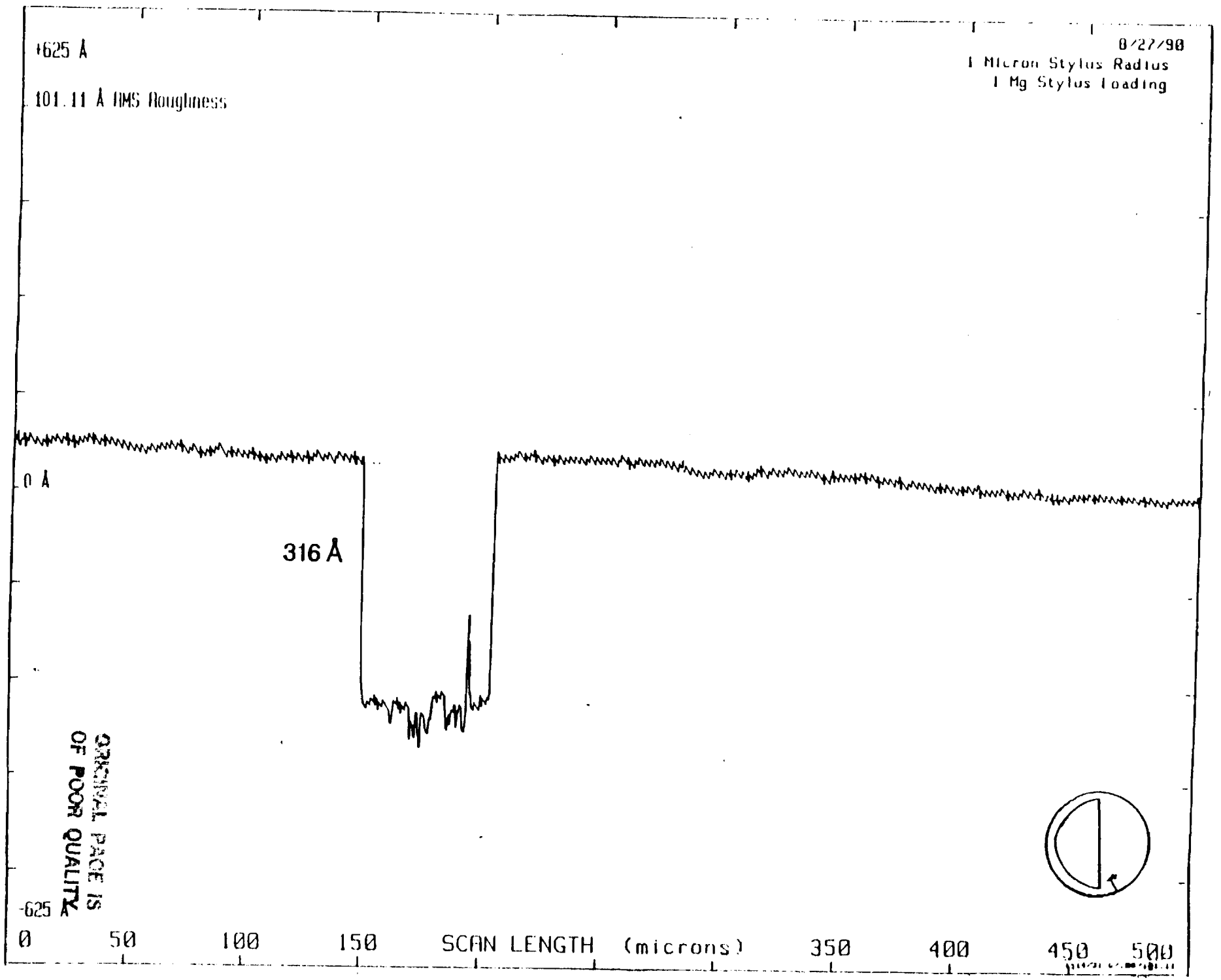

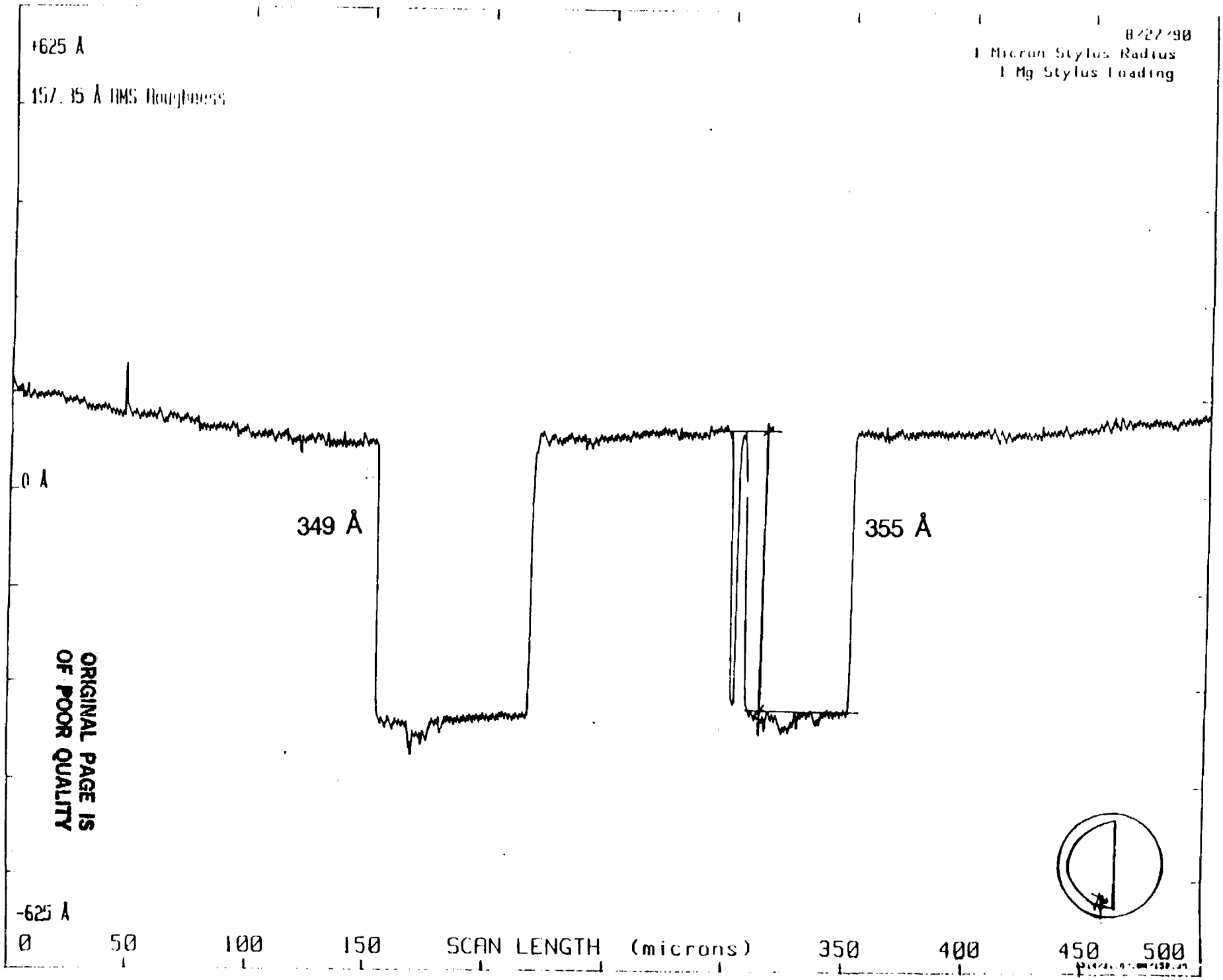

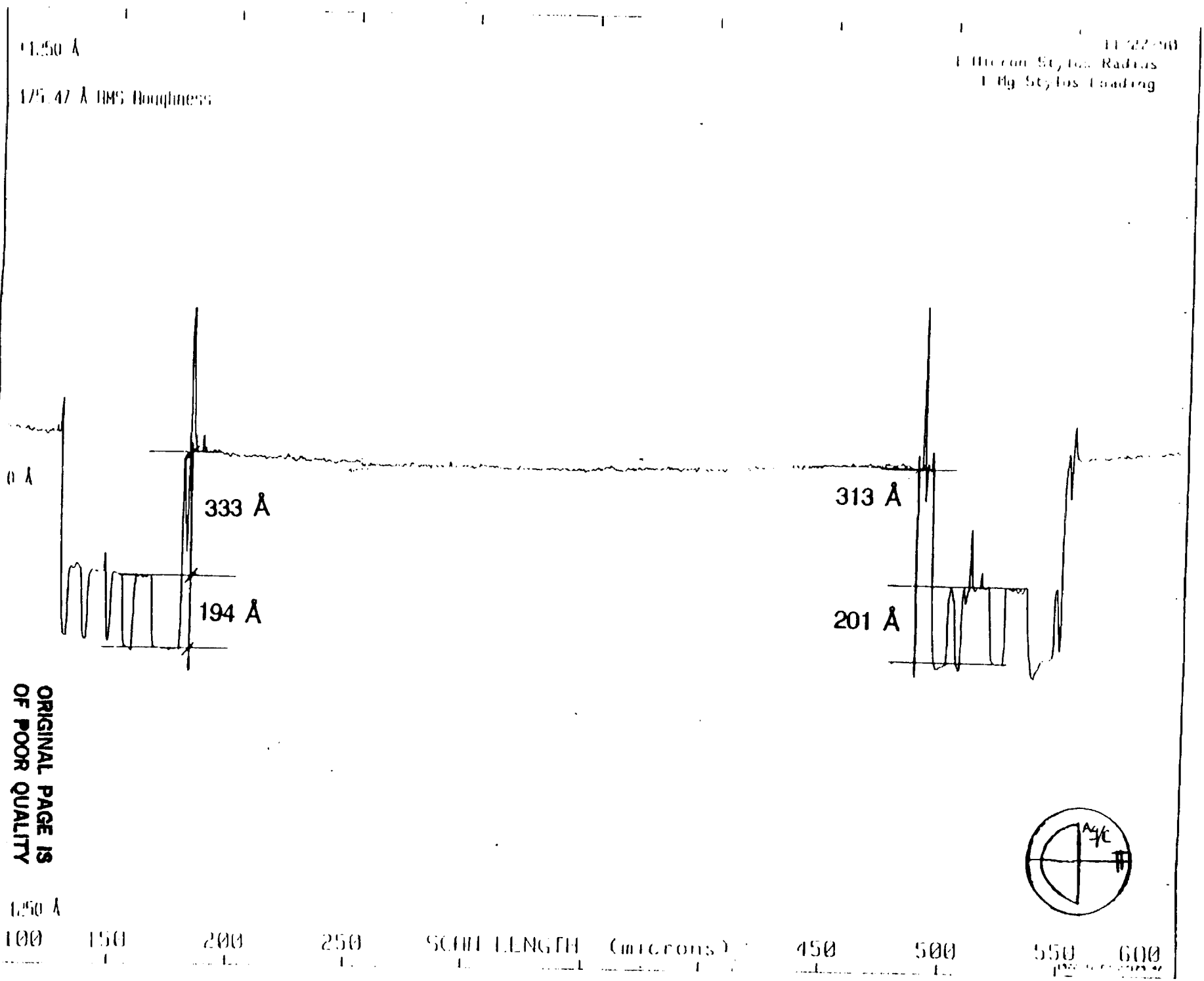

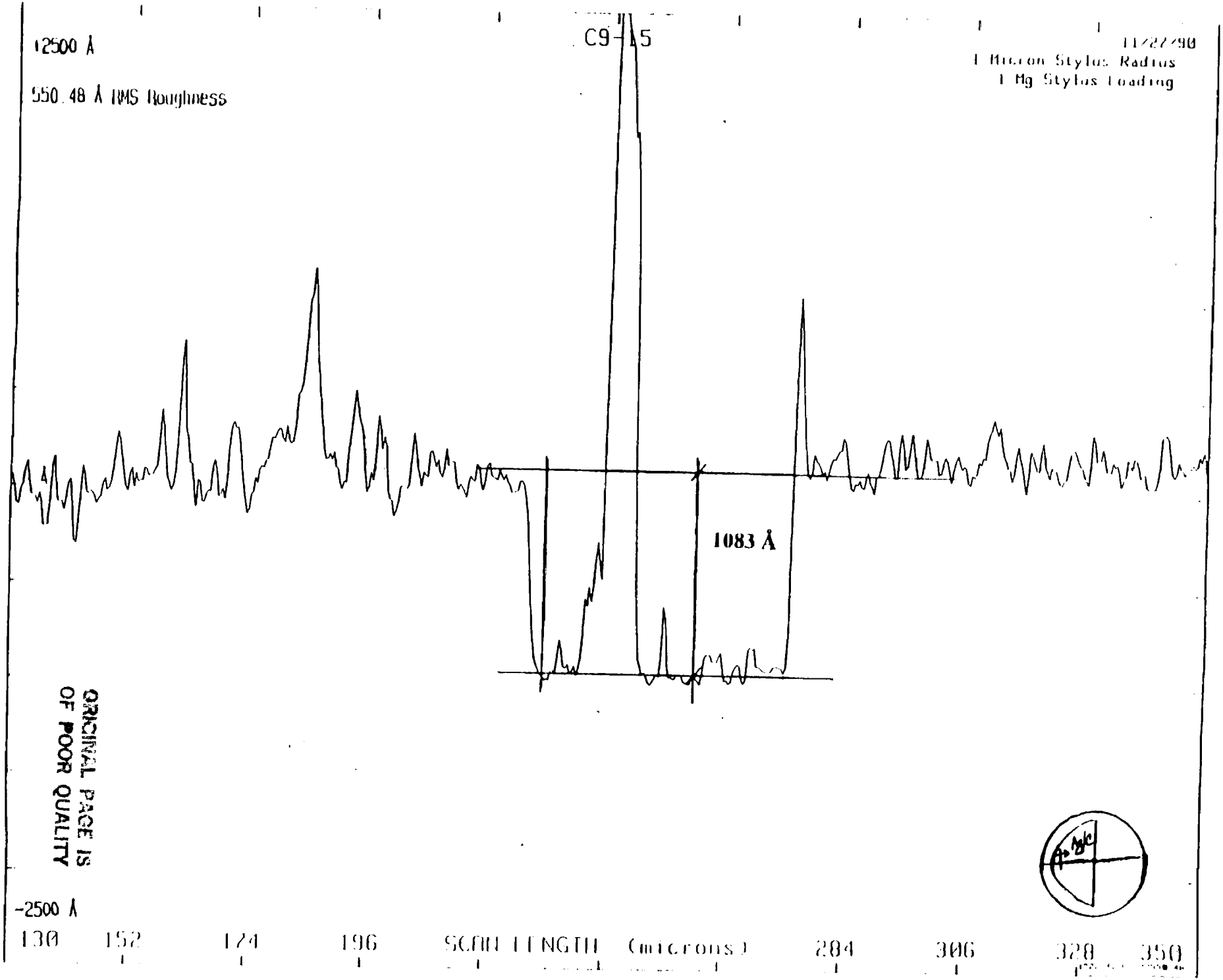

Polycrystalline Carbon (C9-05)

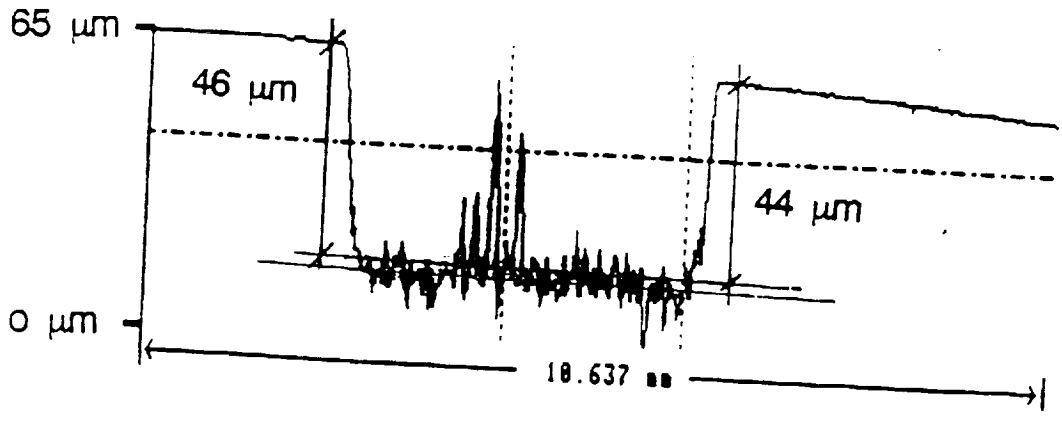

Figure 9. Surface profile of Polycristalline Carbon

PMMA (C9-31)

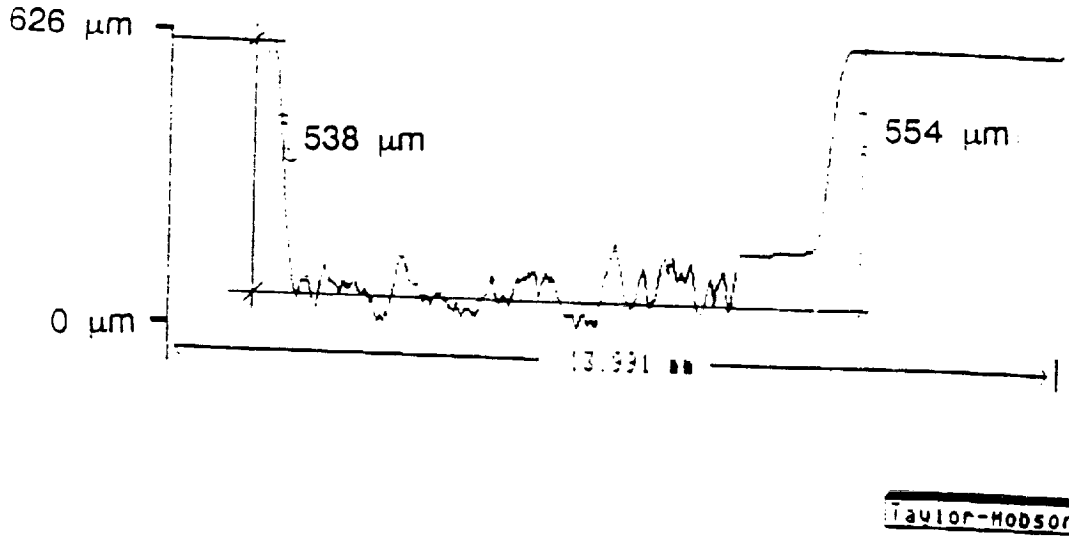

Figure 10. Surface profile of Polymethylmethacrylate at ambient temperature

PMMA (C9H-03)

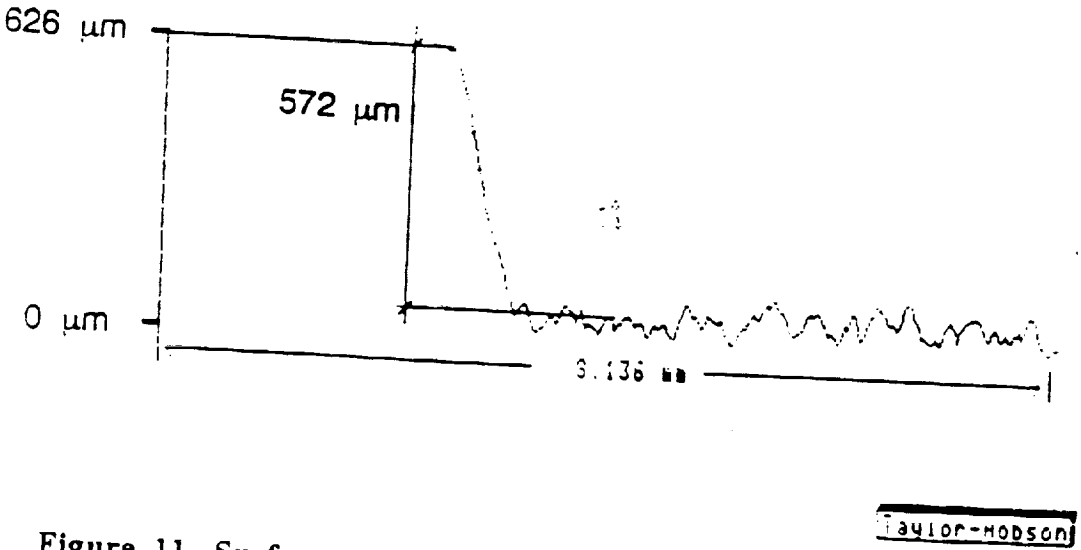

Figure 11. Surface profile of Polymethylmethacrylate at 10^0 C above the ambient temperature

PINHOLE CAMERAS AS SENSORS FOR ATOMIC OXYGEN IN ORBIT; APPLICATION TO ATTITUDE DETERMINATION OF THE LDEF

Palmer N. Peters
Space Science Laboratory, NASA/MSFC
Huntsville, Alabama 35812
Phone: 205/544-7728, Fax: 205/544-7754

John C. Gregory
The University of Alabama in Huntsville*
Huntsville, Alabama 35899
Phone: 205/895-6028, Fax: 205/895-6349

SUMMARY

Images produced by pinhole cameras using film sensitive to atomic oxygen provide information on the ratio of spacecraft orbital velocity to the most probable thermal speed of oxygen atoms, provided the spacecraft orientation is maintained stable relative to the orbital direction. Alternatively, as described here, information on the spacecraft attitude relative to the orbital velocity can be obtained, provided that corrections are properly made for thermal spreading and a co-rotating atmosphere. The LDEF orientation, uncorrected for a co-rotating atmosphere, was determined to be yawed 8.0° ± 0.4° from its nominal attitude, with an estimated ± 0.35° oscillation in yaw. The integrated effect of inclined orbit and co-rotating atmosphere produces an apparent oscillation in the observed yaw direction, suggesting that the LDEF attitude measurement will indicate even better stability when corrected for a co-rotating atmosphere. The measured thermal spreading is consistent with major exposure occurring during high solar activity, which occurred late during the LDEF mission.

INTRODUCTION

A requirement to study the LDEF attitude was identified and a pinhole camera was developed for this purpose as part of Experiment A0114 (refs. 1-3). The atomic oxygen sensitive pinhole camera uses the fact that oxygen atoms dominate the atmosphere in low-Earth orbits, and formation of a nearly

---

*Work supported in part by a grant from UAH Research Institute and NASA grant NAGW-812 and contract NAS8-36645.

collimated beam of oxygen atoms passing through a pinhole in a satellite front surface occurs as a result of the orbital velocity being greater than the most probable Maxwell-Boltzmann speed of the oxygen atoms. Thus, the range of incidence angles of atoms to satellite surfaces is very limited, as shown by the angular distribution curves for two different temperatures in fig. 1 and described in greater detail elsewhere (ref. 4). The same maximum oxygen atom intensity was used for both temperatures to illustrate how the intensity spreads into the wings for higher temperatures. A thin film of material (silver in this case), which is sensitive to atomic oxygen, then forms an image of the impact spot.

The temperature of the thermosphere depends upon solar activity; the 700 K temperature in fig. 1 is characteristic of a solar minimum and the 1500 K is closer to a solar maximum. LDEF altitude was high during the solar minimum of September 1986 (initially deployed at 480 km in April 1984) where oxygen density was lower and had decayed by the time solar maximum was reached in June 1989 (recovery occurred at 310 km in January 1990). Most of the exposure in the pinhole camera, occurred close to solar maximum when the altitude was lower, the oxygen density was greater, and the angular distribution for atom incidence was widest. As will be described later, a well-defined spot was measured on the pinhole camera's silver sensor surface. Although overall darkening from overexposure (scattered atoms within the camera) was observed, this spot has been interpreted as being from the direct incidence beam and was used to determine the orientation of the LDEF relative to the orbital velocity.

MEASUREMENTS

The pinhole camera consisted of a 0.3 mm thick stainless steel hemisphere 3.25 cm (1.28 in.) radius, polished on the concave surface and coated with vacuum-evaporated silver. Silver was used because it discolors from formation of oxide (ref. 5). The pinhole had a conical shape with an included angle much wider than the maximum atom incidence angle and terminated as knife edges at a pinhole diameter of 0.5 mm (0.020 in.). The pinhole was positioned at the center of the silvered hemisphere. As shown in fig. 2, the exposure at any point on the hemisphere will depend upon the solid angle subtended by the pinhole from that point and the point's angular displacement from the orbital direction, i.e., the atom fluence as a function of angle from the velocity vector as shown in fig. 1. For orientations within 10° of the orbital direction, the solid angle subtended by the pinhole is constant within 2%; the predominant effects of pinhole size and thus solid angle are to reduce the overall fluence, or exposure, and increase resolution by reducing pinhole size.

Thus, the spot produced behind the pinhole should be centered with the LDEF's velocity vector and the spot's intensity should correspond to the distribution shown in fig. 1. Any variation in the attitude of the LDEF's velocity vector relative to the atmosphere would cause the spot to wander, producing a nonspherical, larger than normal, spot compared to that produced by thermal spreading of the beam.

Two techniques were used to determine the spot center and its shape: the first technique involved measurements taken directly from an enlarged photograph of the hemisphere taken on-axis with a 120 mm format camera and a 80 mm macro lens, and the second technique involved digitizing a 512 x 512 pixel CCD video camera image of the hemisphere and processing it to obtain both the spot and hemisphere centers and the spot geometry. Both techniques gave similar results.

DISCUSSION

Assuming that misalignment of the pinhole camera relative to the LDEF frame was negligible (machined surfaces and robust structures offer assurance of this), an LDEF orbiting with nominal attitude should have produced a spot centered on the hemisphere and uniformly round. The actual spot, as shown in fig. 3, was off-center, as would be produced by $8^\circ \pm 0.4^\circ$ clockwise yaw viewed from the space end. The spot was elliptical (major axis 14.8° and minor axis 14.1°, as subtended from the pinhole), with the major axis in the satellite yaw direction. It is noted that a yaw of 8° should have narrowed the spot in the yaw direction, not widened it as observed; thus, an oscillation in atom incidence along the yaw direction is the likely cause. This originally led us to conclude that the LDEF oscillated in the yaw direction (i.e., about its long axis), but it has been brought to our attention (Bourrassa, private communication, 1990) that a co-rotating Earth's atmosphere interacting with an inclined orbit produces an oscillation in the angle of incidence of oxygen atoms at the surface. We have verified that the oscillation occurs in the yaw direction, as observed, but the maximum range should be about $\pm 1.5^\circ$, not the estimated $\pm 0.35^\circ$ obtained from the ellipticity measured on the spot. While the center of the spot is rather well defined and is believed to be the average orientation for the LDEF, oscillations, thermal spreading, and other influences on exposure, such as multiple scattering must be separated. Some considerations are:

1. The exposure of the silver was an integrated effect which occurred over 5 3/4 years, over a wide range in oxygen atom temperature, and with an excess background from multiply-scattered atoms. However, most of the oxygen exposure was received during the last six months of the flight.

2. We have not been able to depth profile the exposed silver film, particularly across the spot. Although a nearly circular bulleye pattern suggests a profile similar to those in fig. 1, we have not yet devised a satisfactory technique for measuring optically opaque profiles.

3. Without a depth-composition profile it is not possible to fit the oxygen exposure to a known temperature distribution and there is some uncertainty as to the exact limits of the spot diameter (i.e., where the spot ends and the background takes over); however, it appears that rings on the spot represent equal thicknesses of oxide and provide the measured ellipticity. The minor axis of the spot could represent temperatures as high as 1500 K if assigned FWHM in fig. 1.

4. An oscillating structure and the apparent oscillation caused by an inclined orbit and rotating atmosphere do not yield the same angular flux distribution in a pinhole camera. An oscillating structure sweeps rapidly through the zero displacement and pauses at the extreme angular displacement; The opposite is true for the rotating atmosphere effect. Thus, a mechanical oscillation has a larger integral effect on spot diameter for the same number of degrees of oscillation. We are calculating these profiles with atmospheric oscillations included. Further study is needed to accurately determine the LDEF's range of oscillation.

Analysis by x-ray diffraction of the black powder flaking from much of the camera interior confirmed that it was Ag_2O. For reasons yet unknown, the primary exposed spot was more stable than the rest of the background exposed surface; this assisted our investigation.

AKNOWLEDGEMENTS

The authors are grateful for continued assistance from David Carter, William Kinard, and Jim Jones of the NASA Langley Research Center; to Howard Foulke of the General Electric Company for explanations of their satellite stabilization studies; to William Witherow for digital image measurements; and to Charles Sisk for computer assistance.

REFERENCES

1. Clark, L. G., Kinard, W. H., Carter, D. J., and Jones, J. L., Jr., Eds., "The Long Duration Exposure Facility (LDEF): Mission 1 Experiments," NASA SP-473, Scientific and Technical Information Branch, NASA, Washington, D.C. (1984).

2. Siegel, S. H. and Das, A., "Passive Stabilization of the LDEF," Final Report on contract NASI-13440, GE Document No. 74SD4264, November 1974, General Electric Company, Astrospace Division, Philadelphia, PA.

3. Siegel, S. H. and Vishwanath, N. S., "Analysis of the Passive Stabilization of the LDEF," GE Document No. 78SD4218, August 1977, General Electric Company, Astrospace Division, Philadelphia, PA.

4. Peters, P. N., Sisk, R. C., and Gregory, J. C., "Velocity Distributions of Oxygen Atoms Incident on Spacecraft Surfaces," J. Spacecraft and Rockets, 25(1), 53-58 (1988).

5. Thomas, R. J. and Baker, D. J., "Silver Film Atomic Oxygen Sensors," Can. J. Phys., 50, 1676 (1972).

FIGURE CAPTIONS

Fig. 1. Intensity of oxygen atoms versus incidence angle, cap-theta, in degrees from the orbital ram direction for two equilibrium temperatures of the atoms.

Fig. 2. Schematic of pinhole camera with off-centered spot due to yaw of the LDEF and showing thermal spreading about the spot center due to the effect shown in Fig. 1.

Fig. 3. Photograph of exposed silver hemisphere from pinhole camera; overall dark flaking area is interpreted as overexposure from multi-scattered atoms, and the spot, which is more stable, is believed to be from direct incidence.

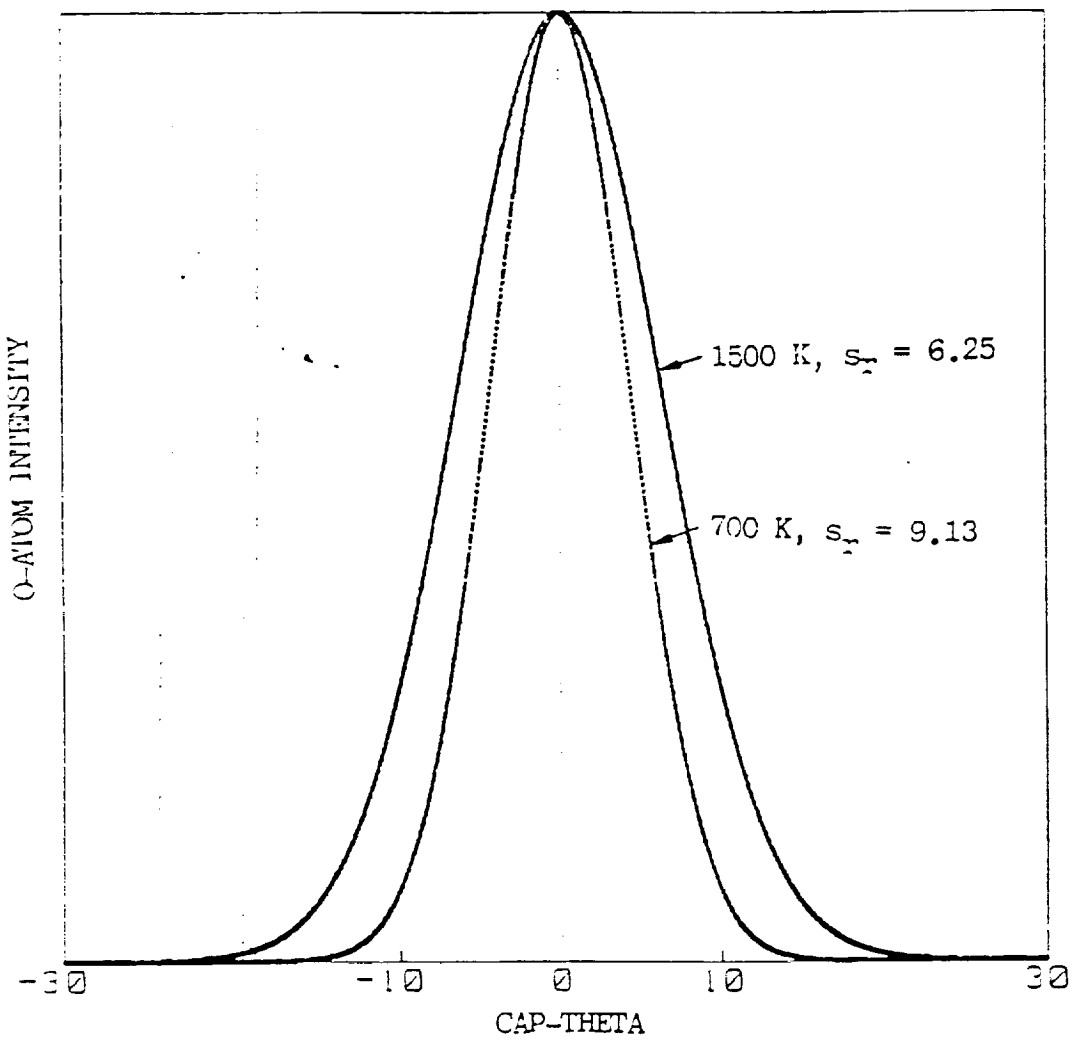
O-ATOM INTENSITY
1500 K, s_T = 6.25
700 K, s_T = 9.13
-30
-10
0
10
30
CAP-THETA

Fig. 1

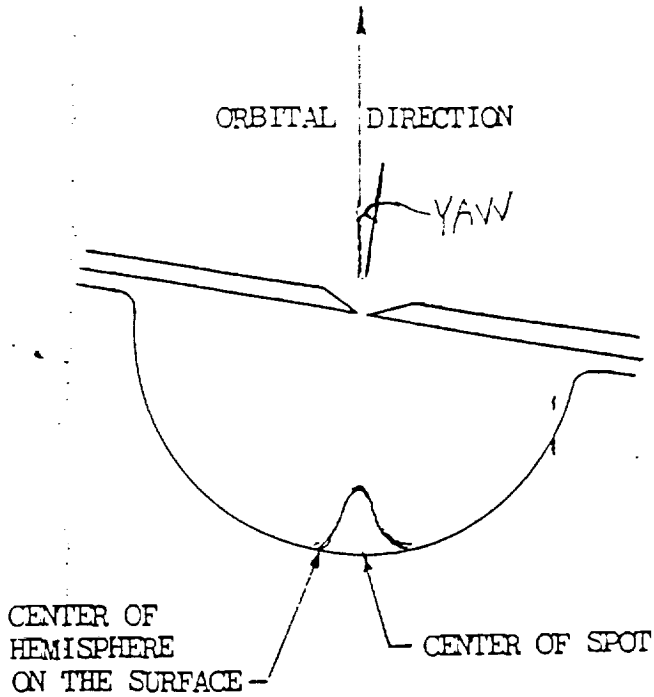
ORBITAL DIRECTION
YAW
CENTER OF
HEMISPHERE
ON THE SURFACE
CENTER OF SPOT

Fig. 2

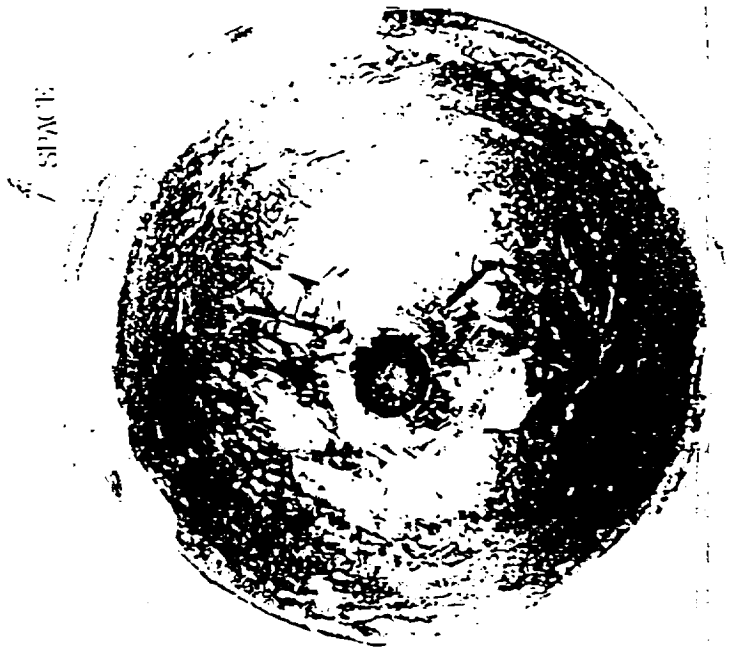

Fig. 3

Measurement of the Passive Attitude Control Performance of a Recovered Spacecraft

J. C. Gregory and P. N. Peters

Reprinted from

Journal of Guidance, Control, and Dynamics

Volume 15, Number 1, January-February 1992, Pages 282-284

AIAA

A publication of the
American Institute of Aeronautics and Astronautics, Inc
The Aerospace Center, 370 L'Enfant Promenade, SW

Measurement of the Passive Attitude Control Performance of a Recovered Spacecraft

J. C. Gregory*
University of Alabama in Huntsville, Huntsville, Alabama 35899
and
P. N. Peters†
NASA Marshall Space Flight Center, Huntsville, Alabama 35812

Introduction

WE report a direct measurement of the attitude-stability of the Long Duration Exposure Facility (LDEF) using a novel silver detector. The University of Alabama in Huntsville (UAH) experiment A-0114, designed primarily to investigate reactions of atmospheric atomic oxygen with materials' surfaces in orbit,[1] also carried a passive device to record the attitude of the vehicle in its orbit. The device showed that the LDEF maintained a very stable attitude during its flight of almost six years. There was a permanent stable offset of 8.0 ± 0.4 deg from nominal in the yaw plane and 1 deg in pitch. The LDEF was a hollow, cylindrical, 12-sided spacecraft, 9.1 m (30 ft) long, 4.3 m (14 ft) in diameter, weighing 9,720 kg (21,400 lb). It was built by NASA Langley Research Center and was launched at an altitude of 480 km by the Space Shuttle Challenger in April 1984 and retrieved by the Columbia in January 1990 at an altitude of 310 km. The spacecraft carried neither a telemetry system nor active attitude measuring and control systems. The facility was designed to stabilize in orbit in the gravity-gradient mode with its long axis parallel to the Earth radius. Predicted rotation about this axis was uncertain.

Background

A long cylindrical object in a circular orbit readily stabilizes about its pitch and roll axes such that its long axis (now that of yaw) is pointing toward the Earth's center. Three-axis stabilization (including the yaw axis) may be achieved if the moments of inertia about the pitch and roll axes differ by a suitable amount. When forced to rotate at orbital rate by gravity gradient torques, a spacecraft will tend to move, that is, rotate about its yaw axis toward the orientation of maximum moment of inertia. The LDEF spacecraft was stabilized in this way by placing weights on the front and back surfaces. In addition, a magneto-viscous damper was used to absorb unwanted angular momentum. This attitude stabilization allowed placement on the LDEF front surface of several experiments to study the effects of atmospheric gases (mostly atomic oxygen at those altitudes) on materials' surfaces. The effects, including erosion of carbon and polymers, corrosion of silver, and oxide film growth on many metals, may be dependent on incidence angle of the gas atoms at the surface. Thus the angular offset of the LDEF attitude in its orbit must be known. Predictions of the capture and attitude stability of the LDEF had been performed,[2,3] including the effects of orbit eccentricity, solar pressure, aerodynamic forces, magnetic dipole, and the magnetically anchored rate damper. Predictions of offsets in pitch, roll, and yaw, and oscillations about these offsets were also made. Although residual damping torques from the magnetic damper were not negligible after attitude stability was achieved, the predicted offsets were dominated by aerodynamic forces. These result when the center of mass of the spacecraft does not coincide with the center of pressure (assumed to be at the geometric center). Displacement of these centers along the yaw axis (local vertical) results in pitch offset, and displacement along the pitch axis results in yaw. The yaw offsets and uncertainties are much larger since the restoring torques are two orders of magnitude less than those for pitch. Predicted maximum offset angles for the final configuration were 1 to 2 deg in pitch and up to 30 deg in yaw.[3] Roll errors were small but in any event unmeasurable by the UAH device.

Experimental Measurement

The atmosphere at altitudes of several hundred kilometers consists predominantly of oxygen atoms produced by dissociation of O_2 molecules by solar ultraviolet photons. As a satellite moves through this thin but chemically reactive atmosphere, oxygen atoms impinge on its front surface at satellite velocity (approximately 8 km/s), modified somewhat by the random thermal velocities of the atoms themselves. The sensing device uses the property of silver to adsorb oxygen atoms with high efficiency, being converted to silver oxide. The optical appearance, transmission, reflectivity, and electrical properties of silver films are drastically changed during this process. The phenomenon has been used to measure atomic oxygen concentration on sounding rockets[4] and to measure

Received Sept. 10, 1990; revision received Oct. 25, 1990; accepted for publication Oct. 25, 1990.

*Professor of Chemistry and Materials Science, Department of Chemistry.
†Physicist, Mail Code ES 63, Space Science Laboratory.

the angular distribution of 5 eV (8 km/s) oxygen atoms scattered from a solid surface in low Earth orbit.[5] This is the first application of the technique to attitude sensing on orbital vehicles.

The device consisted of a hemispherical stainless steel cup, radius 32.5 mm (1.28 in.), coated on the inside surface with an evaporated Ag film 5 μm thick. The cup, facing forward in the nominal orbital direction, was mounted behind a plate with a hole, 0.5 mm (0.020 in.) in diameter, positioned at the center of the hemisphere. This aperture admitted the atomic oxygen flux into the device during the entire 5.75 years of the flight, though the planned duration was only 10 months. Though the silver film was severely overexposed, nevertheless the impact zone of the orbital-velocity oxygen atoms on the film is clearly evident in Fig. 1. During the flight, it is estimated that 2×10^{19} oxygen atoms entered the device. These atoms diverged from the orifice with an angular distribution dependent on gas temperature and satellite velocity as previously described.[6] They struck a zone on the hemisphere approximately 0.8 cm in diameter. This provided a dose of 4×10^{19} atoms cm^{-2} to the Ag film in this zone, enough to heavily oxidize the film. Oxygen atoms were then diffusely reflected by the Ag_2O surface and again off the back of the aluminum mounting plate. Since the entire Ag film in the detector was heavily oxidized, as clearly seen in the photograph, recombination of atoms to O_2 (which does not significantly react with Ag) is not a dominant process. There was evidence of fresh silver revealed behind portions of peeled Ag_2O film. Though all portions of the film have received large doses of atomic oxygen, the area struck by the fast atoms entering the device is qualitatively different and produced a visible elliptical spot of more adherent oxide seen in Fig. 1. The dimensions of this spot are shown diagrammatically in Fig. 2, and its offset with respect to the center of the circle, which is the projection of the detector hemisphere, were recorded. The device was placed on the spacecraft so that if the attitude of LDEF had been nominal, the oxidation spot would have been in the center of the disk. Angular offset of the vehicle from nominal results in an equal angular displacement of the centroid of the spot from the center of the disk. The size and shape of the spot are related to both the temperature of the orbital gas and to the stability of the vehicle about its mean position. Oscillation about either yaw or pitch axis would cause elongation of the spot in orthogonal directions. The viewer sees both Figs. 1 and 2 in the same sense, looking backward along the velocity vector, as if looking at the inside of the cup through the small aperture in the front plate. The point (0,0) in Fig. 2 is the center of the flat projection of the hemispherical cup, while (p,q) is the geometric center of the elliptical oxide spot observed. If the orientation of LDEF had been perfect, (p,q) and (0,0) would have coincided.

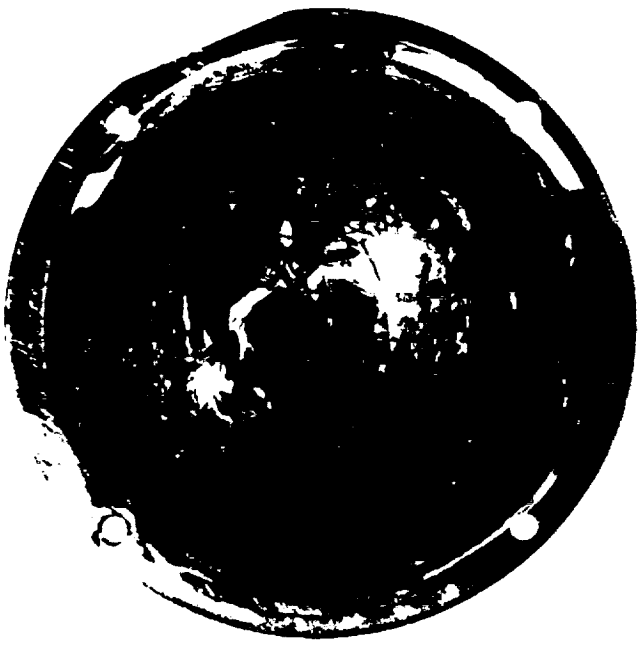

Fig. 1 Photograph (plan view) of the exposed attitude-measuring device after retrieval from orbit. The impact zone of the orbital velocity oxygen atoms is visible as an ellipse slightly off center.

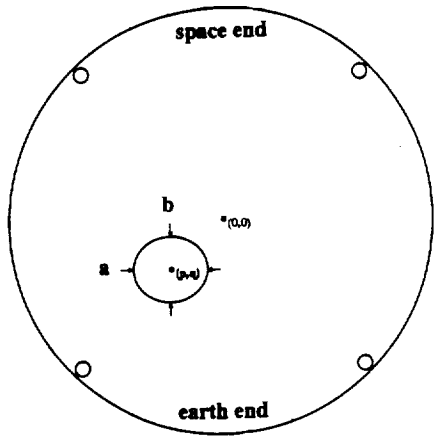

Fig. 2 Diagrammatic representation of Fig. 1 showing the coordinates referred to in Table 1.

Measurements were made in two ways. The silver cup was directly viewed with a digital image analysis system using a 512 $\times$ 512 CCD camera. The centroid of the circular image of the cup was found, and its separation from the centroid of the slightly elliptical spot was measured. In the second method, a photographic image of Fig. 1 (made with a Mamiya 645 camera and 80 mm Macro lens) was directly measured. The combined results are shown in Table 1. Corrections for curvature were insignificant over the angular range of interest and were not included.

Discussion

Before the size and shape of the spot produced on the silver film in our device may be used to estimate the motions of the spacecraft about its center of mass, we must establish the broadening due to thermal motions of the gas atoms. The angular dispersion of atoms passing through an orifice in an orbiting plate has been calculated as a function of temperature by Peters et al.[6] and is shown in Table 2. The effect of temperature is shown here in the speed ratio S_r, which relates the satellite speed to the most probable Maxwell-Boltzmann speed of the atoms. The width of the angular distribution of atoms passing through an orifice in a plate under these conditions increases markedly with temperature. Gas temperatures at orbital attitudes vary strongly with cyclical solar activity. LDEF was in orbit for a full half solar cycle during which the mean gas temperature may have varied over the range of 700–1500 K, corresponding to angular distributions of 10.4–15 deg. We believe that the minor diameter of the elliptical spot (14.1 deg) is consistent with the gas temperature during the flight, and no evidence exists for broadening caused by significant instability in the spacecraft pitch plane.

The observed ellipticity (1.05) with the major axis in the satellite yaw plane indicates an instability of 0.4 $\pm$ 0.15 deg

Table 1 Measured coordinates and ellipticity of the oxygen atom impact zone [the point (0,0) is at the center of the device]

Coordinates of spot centroid (p,q)		Major, minor axes of spot (a,b)
10^{-3} in.	deg	deg
$-(178 \pm 8, 21 \pm 8)$	$(8.0 \pm 0.4, \quad 1.1 \pm 0.4)$	(14.8, 14.1)

Table 2 Calculations of the angular distribution function for oxygen atoms passing through an orifice in an orbital plane at various gas temperatures

Temperature, K	Speed ratio,[a] s_r	Angular width FWHM,[b] deg
600	9.87	9.60
700	9.13	10.36
800	8.54	11.06
900	8.06	11.70
1000	7.64	12.32
1100	7.29	12.90
1200	6.98	13.44
1300	6.70	13.97
1400	6.46	14.48
1600	6.04	15.44
1800	5.70	16.32
2000	5.40	17.16

[a]The speed ratio of the satellite velocity (with respect to a stationary atmosphere) taken here as 7.77 km/s to the most probable speed for a Maxwell-Boltzmann distribution for O atoms at the given temperature.
[b]Full width at half maximum.

(full width) in this plane over a significant portion of the orbital exposure.‡ Since the detector system records all angular instabilities on top of one another, time-dependent instabilities cannot be resolved. The result is weighted by oxygen-atom exposure rather than just time averaged. Since the O atom density is exponential with decreasing altitude and the LDEF descended in its orbit at an increasing rate, the bulk of the oxygen exposure was accumulated during the last few months before capture. However, the attitude instabilities themselves are most likely to have been caused by aerodynamic forces. These were also at maximum during the latter portion of the flight as the satellite entered the denser regions of the atmosphere. Thus, the yaw instability of ±0.2 deg may only have occurred late in the flight.

Conclusions

Evidence from the passive attitude detector on experiment A0114 showed that the LDEF spacecraft maintained a highly stable attitude during its 5.75-year flight. There was a small offset yaw of 8.0 ± 0.4 deg clockwise from nominal attitude as viewed from space. There also appeared to be an oscillation of ±0.2 deg about this offset yaw.‡ The satellite was pitched slightly forward by about 1 deg (space end leading). Those experiments on the LDEF that depend on orientation relative to the forward direction, such as atomic oxygen reaction cross-section measurements, may need to be corrected for the angular offset. The gravity-gradient mode of spacecraft stabilization has great cost benefits over those using active systems, particularly for long-lived missions, but uncertainty in yaw stability has been a concern for many applications. With demonstration of the high degree of stability about the yaw axis experienced by the LDEF, the instabilities predicted for passively stabilized spacecraft may be reduced.

‡It has been observed[7] that the corotation of the atmosphere with the Earth itself would produce a deviation of ±1.5 deg in incidence angle of the atmosphere with the LDEF front surface as it crossed the equator. Such an effect, which we believe to be real, would be indistinguishable from an oscillation in yaw.

Acknowledgments

The authors are grateful for continued assistance from David Carter, William Kinard, and Jim Jones of the NASA Langley Research Center over the extended lifetime of this project; to Howard Foulke of the General Electric Company for explanations of their satellite stabilization predictions; and to William Witherow for digital image measurement. The instrument was built with a grant from the UAH Research Institute and data analysis at UAH was supported in part by NAGW-812 and NAS8-36645.

References

[1]Clark, L. G., Kinard, W. H., Carter, D. J., and Jones, J. L., Jr. (eds.), "The Long Duration Exposure Facility (LDEF): Mission 1 Experiments," Scientific and Technical Information Branch, NASA, NASA SP-473, Washington, DC, 1984.

[2]Siegel, S. H., and Das, A., "A Passive Stabilization of the LDEF," General Electric Company, Final Report on contract NASI-13440, GE Document No. 74SD4264, Astrospace Division, Philadelphia, PA, Nov. 1974.

[3]Siegel, S. H., and Vishwanath, N. S., "Analysis of the Passive Stabilization of the LDEF," General Electric Company, GE Document No. 78SD4218, Astrospace Division, Philadelphia, PA, Aug. 1977.

[4]Thomas, R. J., and Baker, D. J., "Silver Film Atomic Oxygen Sensors," *Canadian Journal of Physics*, Vol. 50, 1972, p. 1676.

[5]Gregory, J. C., and Peters, P. N., "A Measurement of the Angular Distribution of 5eV Atomic Oxygen Scattered Off a Solid Surface in Earth Orbit," *Rarefied Gas Dynamics*, edited by V. Boffi and C. Cercignani, Vol. 15, No. 1, 1986, p. 644-656.

[6]Peters, P. N., Sisk, R. C, and Gregory, J. C., "Velocity Distributions of Oxygen Atoms Incident on Spacecraft Surfaces," *Journal of Spacecraft and Rockets*, Vol. 25, No. 1, 1988, pp. 53-58.

[7]Bourrassa, R., The Boeing Company, private communication, June 1991.

Letters to Nature

combined with lack of evidence of extensive spontaneous internalization of cell-surface class II molecules, suggested that these are newly synthesized MHC proteins on their way to the surface. The findings implied that class II MHC molecules are present from the earliest contact between antigen and the cellular processing machinery, and may potentially bind antigenic peptides as soon as they become available, shielding them for further degradation[12,13].

Such early rendezvous of class II MHC and antigen was not observed by Peters *et al.*[1]. Although agreeing that it is newly synthesized class II molecules rather than those recycled from the cell surface that are detected in the endocytotic system, they find that class II MHC proteins in the endocytotic pathway are confined primarily to structures resembling lysosomes; that is, much further along the pathway than early endosomes. According to this picture, endocytosed antigens must run nearly the full gamut of acid pH and endosomal proteolysis before having the opportunity to bind class II molecules, suggesting that antigenic peptides would have to be hardy survivors of the endosomal degradative system. In this regard, Peters *et al.* observed that it took 20–50 minutes for a proteolytically resistant endocytosed molecule to reach the lysosome-like compartments containing class II molecules; meanwhile, the more readily degraded bovine serum albumin molecule was detected there only poorly, implying that proteolysis takes its toll of material moving in to deeper structures.

Clearly, there are labile T-cell determinants that are not presented well from endocytosed antigens[14] or whose presentation is markedly enhanced by inhibition of cellular proteolytic activity[15,16]. Whether this functional degradation of T-cell determinants observed in biological assays results from a prolonged trip towards class II MHC in an increasingly harsh endosomal environment requires direct information; failure to detect molecules by electron microscopy does not necessarily mean that T-cell epitopes could not be pulled from the digest by MHC molecules. Further, although the lag period of 30–60 minutes needed for endocytosed antigen to become available for T-cell recognition[17] fits neatly with the time taken by antigen to travel to the lysosome-like MHC-containing structures, it is not established that this is the rate-limiting step in antigen presentation. On the other hand, the observation by Peters *et al.* that intracellular class II MHC molecules have half-lives of hours may explain why antigen presentation can persist for hours after cellular protein synthesis has been inhibited[18].

How can the findings of Guagliardi *et al.*[11] and Peters *et al.*[1] be reconciled? Information is needed on how results could be affected by use of different cell lines, or cells cultured under different conditions. The degree of resolution of molecules is also a consideration, but here one would expect that the thawed cryosections used by Peters *et al.* would be more sensitive than the plastic-embedded material of Guagliardi *et al.* In any event, no technique has yet revealed where the association between antigen and class II molecules actually occurs. Experiments addressing functional association — that is, experiments using T-cell recognition — will probably be required in order to resolve this issue.

There are also pressing questions on the related immunology. For instance, is there a way by which endogenously synthesized antigens (for a review see ref. 19) could enter a compartment to associate with class II MHC, other than by uptake at the cell surface? Are there mechanisms in the class II/antigen presentation system similar to those uncovered for class I, such as molecules which actively translocate peptides to compartments for MHC association, or the need to form a complex with antigen as a prerequisite for transport of MHC to the cell surface? Finally, can the observation that protein antigens are presented by intact antigen-presenting cells faster and at much lower concentrations than expected from studies with isolated molecules[20] be explain by how peptide and MHC meet in specialized intracellular compartments? □

Charles J. Hackett is at The Wistar Institute, 36th and Spruce Streets, Philadelphia, Pennsylvania 19104, USA.

1. Peters, P.J., Neefjes, J.J., Oorschot, V., Ploegh, H.L. & Geuze, H.J. *Nature* **349**, 669–676 (1991).
2. Yewdell, J.W. & Bennink, J.R. *Cell* **62**, 203–206 (1990).
3. Parham, P. *Nature* **348**, 674–675 (1990).
4. Townsend, A. *et al. Nature* **340**, 443–448 (1989).
5. Teyton, L. *et al. Nature* **348**, 39–44 (1990).
6. Bakke, O. & Dobberstein, B. *Cell* **63**, 707–716 (1990).
7. Neefjes, J.J., Stollorz, V., Peters, P.J., Geuze, H.J. & Ploegh, H.L. *Cell* **61**, 171–183 (1990).
8. Gruenberg, J. & Howell, K.E. *A. Rev. cell. Biol.* **5**, 453–481 (1989).
9. Griffiths, G., Back, R. & Marsh, M. *J. Cell Biol* **109** 2703–2720 (1989).
10. Blum, J.S. & Cresswell, P. *Proc. natn. Acad. Sci. U.S.A.* **85**, 3975–3979 (1988).
11. Guagliardi, L.E. *et al. Nature* **343**, 133–139 (1990).
12. Loyse-Cobian, F. & Urbanus, E.R. *J. Immun.* **143**, 1445–1450 (1989).
13. Wandelin, O. *Scand. J. Immun.* **31**, 625–636 (1990).
14. Eisenlohr, L.C. & Hackett, C.J. *J. exp. Med.* **169**, 921–931 (1989).
15. Buus, S. & Wandelin, O. *J. Immun.* **138**, 452–453 (1988).
16. Grodehandt, G., Hampl, J., Milbradt, S. & Rude, E. *Eur. J. Immun.* **20**, 2637–2641 (1990).
17. Roosnek, E. *et al. J. Immun.* **140**, 4079–4082 (1988).
18. St-Pierre, Y. & Watts, T.H. *J. Immun.* **148**, 812–818 (1990).
19. Long, E.O. *Immun. Today* **10**, 232–234 (1989).
20. Sadegh-Nassen, S. & McConnell, H. *Nature* **337**, 272–276 (1989).

Come in LDEF, your time is up

THE first satellite to be recovered by a space shuttle, the Long Duration Exposure Facility (LDEF) was retrieved by Columbia on 12 January 1990. It is seen here in its last moments in free-fall. LDEF was launched in 1984 to study the effects of cosmic dust and rays. The experiment reported by Fishman *et al.* on page 678 of this issue may indicate the kind of surprises in store for participants in the project. Amongst the gases and ions swept up by LDEF during its mission were prodigious quantities of beryllium-7. Produced by cosmic-ray interactions with air at an altitude of 40 km, 270 km below LDEF's orbit, ^{7}Be has a half-life of only 53 days, so that the authors are at a loss to explain how it came to be trapped by the satellite. □

18. Volkoya, E. et al. Astr. Astrophys. 208, 1–20 (1988).
19. Shimizu, H. et al. Publ. astr. Soc. Jpn 40, 665–671 (1988).
20. Ellerbroek, A. P. & Rose, W. K. Astrophys. J. 208, 114–127 (1988).
21. McNally, I. M. in Proc. IX. Lec Objects (eds Maruschi, L., Maccacaro, T. & Ulrich, M.-H.) 189–196 (Springer, Berlin, 1988).
22. Marscher, A. P. Astrophys. J. 264, 296–297 (1983).
23. Zensus, J. A. in Proc. IX. Lecp Objects (eds Maraschi, L., Maccacaro, T. & Ulrich, M.-H.) 3–12 (Springer, Berlin, 1988).
24. Lind, K. R. & Blandford, R. D. Astrophys. J. 295, 358–367 (1985).
25. Hughes, P. A., Aller, H. D. & Aller, M. F. Astrophys. J. 298, 301–315 (1985).
26. Stocke, J. T. in Proc. IX. Lec Objects (eds Maraschi, L., Maccacaro, T. & Ulrich, M.-H.) 456–459 (Springer, Berlin, 1988).
27. Bignall, F., Gioiangia, E. & Cavaliere, A. Astrophys. J. (in the press).

ACKNOWLEDGEMENTS. I thank John Peacock for many helpful comments and suggestions.

Observation of ^{7}Be on the surface of LDEF spacecraft

G. J. Fishman*, B. A. Harmon†, J. C. Gregory‡, T. A. Parnell*, P. Peters*, G. W. Phillips§, S. E. King§, R. A. August§, J. C. Ritter§, J. H. Cutchin‖, P. S. Haskins¶, J. E. McKisson+, D. W. Ely+, A. G. Weisenberger+, R. B. Piercey** & T. Dybler**

* Space Science Laboratory, Code ES62, NASA Marshall Space Flight Center, Alabama 35812, USA
† Universities Space Research Association, Huntsville, Alabama 35806, USA
‡ Department of Chemistry, University of Alabama in Huntsville, Huntsville, Alabama 35899, USA
§ Naval Research Laboratory, Washington, DC 20375-5000, USA
‖ Sachs/Freeman Associates, Washington, DC 20375-5000, USA
¶ University of Florida, Gainesville, Florida 32609, USA
+ Institute for Space Science and Technology, Gainesville, Florida 32609, USA
** Department of Physics, Mississippi State University, Mississippi State, Mississippi 39762, USA

THE Long Duration Exposure Facility (LDEF), an orbiting unmanned satellite, was recently returned to Earth after almost six years in space. From radioactivity measurements, we have found significant quantities of the isotope ^{7}Be on the leading edge (but only on the leading edge) of LDEF. Although the absolute atmospheric concentration of ^{7}Be needed to explain this detection is extremely small (10^{-7} atoms cm^{-3}), its concentration at LDEF's altitude (310 km) must be several orders of magnitude higher than in the stratosphere below, where it is produced by cosmic-ray reactions with atmospheric nitrogen and oxygen nuclei. To explain the presence of ^{7}Be on the surface of LDEF, it must first be rapidly and efficiently transported to high altitudes, and then adsorbed onto the surface of the spacecraft. Neither process had been expected. Our detection may therefore lead to the use of ^{7}Be as an exo-atmospheric tracer, as well as to studies of surface interactions in space.

The LDEF spacecraft was launched by the space shuttle Challenger on 7 April 1984 into a nearly circular orbit with an inclination of 28.5° and an altitude of 480 km. It was retrieved by the space shuttle Columbia on 12 January 1990 at an altitude of 310 km. Because of its large mass, long space exposure and the wide variety of materials onboard, the LDEF provided a unique opportunity for induced radioactivity studies. These measurements are still in progress and will be reported elsewhere.

The LDEF spacecraft is a twelve-sided cylindrical aluminium structure, 9.1 m long by 4.3 m in diameter (see Fig. 1). It consists of an open grid to which were attached various experiment trays designed to measure the effects of long space exposure on spacecraft materials and components. Throughout its orbital lifetime, the spacecraft was passively stabilized about all three axes of rotation, allowing one end of the spacecraft to point always toward the Earth, and fixed leading and trailing sides with respect to the orbital motion.

After its return to the Kennedy Space Center, gamma-ray spectra were obtained along each side of the spacecraft using a germanium detector array provided by the Naval Research Laboratory. Measurements were also made of selected components from the spacecraft. The gamma-ray line at 478 keV from the radioactive decay of ^{7}Be was unambiguously observed to emanate from the leading side of the spacecraft, as shown in Fig. 1. The weaker signal observed from the trailing side of the spacecraft can be traced to the attenuated gamma-ray flux from the leading surfaces.

Individual components were brought to the Marshall Space Flight Center to quantify the residual radioactivity on the LDEF. A high-purity germanium detector inside a low-level background facility was used to obtain spectra of small aluminium and steel samples taken from the leading and trailing sides. In Figs 2 and 3, gamma-ray spectra of two identical aluminium plates and two steel trunnion end pieces taken from the leading and trailing sides of the spacecraft are shown. A clear ^{7}Be signal was seen on the leading side, with little or no signal above background on the trailing side.

A polished aluminium plate, used as a thermal control surface in LDEF experiment AO114 (ref. 1), was subjected to several tests to determine the depth of penetration and the form of deposition of the ^{7}Be. The surface was coated with collodion, stripped to remove all loose particles, then wiped firmly with xylene. Less than 10% of the surface activity was removed by this process, indicating that the ^{7}Be was neither associated with dust particles nor other soluble surface contaminants. An acid etch, without a stable beryllium carrier, removed several tens of micrometres of the aluminium surface, and most of the ^{7}Be activity (the remainder was assumed to be re-deposited). This suggests that the ^{7}Be ions are trapped in the metal oxide surface layer, indicative of a chemical interaction with the surface. Such a process was previously unknown, with the exception of the atomic oxygen effect[1].

In Table 1, the measured number of ^{7}Be atoms per unit area on various spacecraft surfaces is shown. The results are corrected to the retrieval date of 12 January 1990 and for the offset angle from the leading direction. The areal density for ^{7}Be on the aluminium and steel is the same within the experimental uncertainty, and is apparently not a strong function of the type or surface condition of the metal. The Teflon thermal coating, however, which was used on many LDEF experiment trays, has a density of ^{7}Be an order of magnitude lower than that found on the aluminium surface. The reason for this apparent difference in uptake efficiency is unknown, but could be related to the material's covalence-bond structure. The explanation may be complicated, also, by the observed erosion of the Teflon surface by atomic oxygen.

The appearance of ^{7}Be on the leading surfaces, as shown in Figs 1–3, rules out direct production of the isotope within the spacecraft by the incident radiation flux. In striking contrast to the distribution of ^{7}Be, the increased flux of geomagnetically trapped protons from the west in this type of orbit[2] results in higher spallation-induced activities on the trailing side of the spacecraft (see Figs 2 and 3). Such induced activity is also not

TABLE 1 LDEF ^{7}Be surface concentrations

Material	^{7}Be areal density ($\times 10^{6}$ atoms cm^{-2})
Stainless steel trunnion face	5.3 ± 0.7
Polished aluminium plate Exp. AO114	6.7 ± 1.0
Anodized aluminium experiment tray clamp	4.6 ± 0.5
Teflon thermal cover	0.9 ± 0.2

Corrected for decay since recovery and for surface orientation relative to spacecraft ram direction.

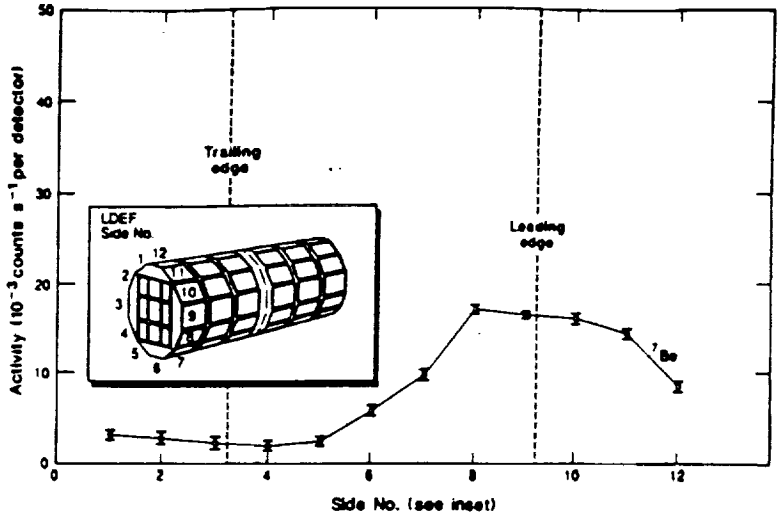

FIG. 1 The activity of ^{7}Be measured from the twelve sides of the LDEF spacecraft at the Kennedy Space Flight Center, corrected to the date of retrieval.

confined to the surface. Although we do observe a small ^{7}Be signal from aluminium samples taken from the trailing side of the spacecraft, this contribution is at a level we expect from reactions with the incident flux, and is about two orders of magnitude smaller than the surface activity of the leading side. This leads us to conclude that the ^{7}Be must have accumulated on the spacecraft surfaces from the ambient atmosphere at orbital altitudes.

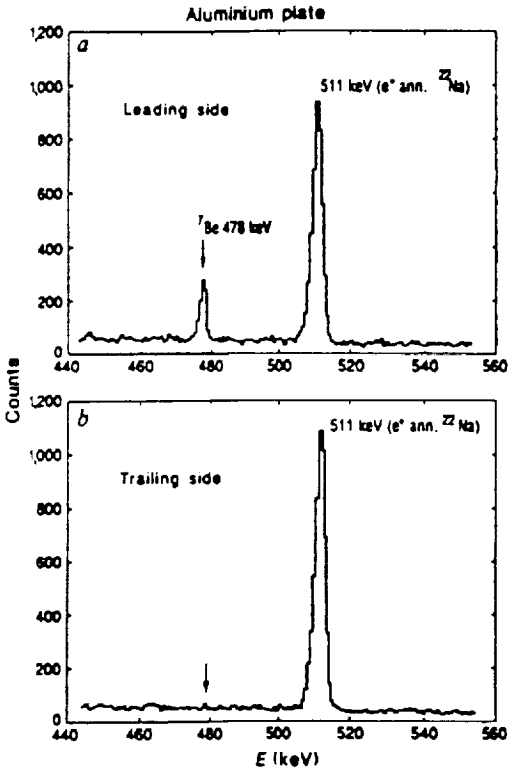

FIG. 2 Gamma-ray spectra of aluminium plates on the leading and trailing sides of LDEF. The isotope ^{7}Be is identified by the strong line at 478 keV seen on the leading side but not on the trailing side. The strong line at 511 keV is produced by positron-annihilation gamma rays from the spallation product ^{22}Na, as well as laboratory background. Both spectra represent 48-h counts.

The short-lived isotope ^{7}Be was first detected in the atmosphere by Arnold and Al-Salih in 1955[3], and later mapped by others as a function of altitude and latitude[4–8]. It is produced in the atmosphere by high-energy cosmic-ray interactions with air as are other radioisotopes such as ^{14}C and ^{3}H. Once formed, ^{7}Be ions are presumed to oxidize rapidly and attach to small aerosol particles, providing a downward transport mechanism from peak production regions of the atmosphere[9–14]. The primary removal process for ^{7}Be, which occurs on a timescale comparable to its mean lifetime (~77 days), is the washout of the aerosol-attached ^{7}Be in rain water[3–6].

At a given latitude above ~20 km, the production rate of ^{7}Be varies vertically in proportion to the oxygen-nitrogen gas density. Peak production per unit volume occurs in the lower stratosphere, at ~20 km, below which the cosmic-ray flux is substantially attenuated. At higher altitudes, the number of ^{7}Be atoms produced per unit volume decreases rapidly, but the number of ^{7}Be atoms per unit mass of air, or concentration, should be essentially constant. Balloon and aircraft measurements[4,15] are in approximate agreement with this, although few measurements extend much above the peak production altitudes.

We can calculate the concentration of ^{7}Be at 310 km from the data in Table 1, assuming the trapping efficiency on the metal surfaces is near unity. Using the LDEF orbital velocity of 7.8 km s^{-1} and the 77-day mean lifetime of ^{7}Be, we find a density of 1.1×10^{-7} atoms cm^{-3}, or a relative concentration of 3.8×10^6 atoms per gram of air. In the peak production region, at altitude 20 km, previous measurements[4–8] yield a concentration of 10^3 ^{7}Be atoms per gram of air, or ~0.1 atoms cm^{-3}, in agreement with a simple calculation using the known cosmic-ray flux. Thus, the measured concentration of ^{7}Be per unit mass of air at 310 km is three to four orders of magnitude in excess of the concentration at 20–50 km.

The concentration of ^{7}Be in the 300-km range, far in excess of what can be produced in air at that altitude, is evidence of an unknown mechanism transporting ^{7}Be from the stratosphere. Although the amount being transported (or removed) from the peak production regions is a minute fraction of the total atmospheric burden of ^{7}Be, the observed density is contrary to assumptions of conventional atmospheric transport and mixing, and in particular, to the assumed attachment to aerosol particles[16]. Whatever the mechanism, however, the transport to orbital altitudes must take place on a timescale similar to the mean lifetime of ^{7}Be.

Systematic low-level induced radioactivity measurements of

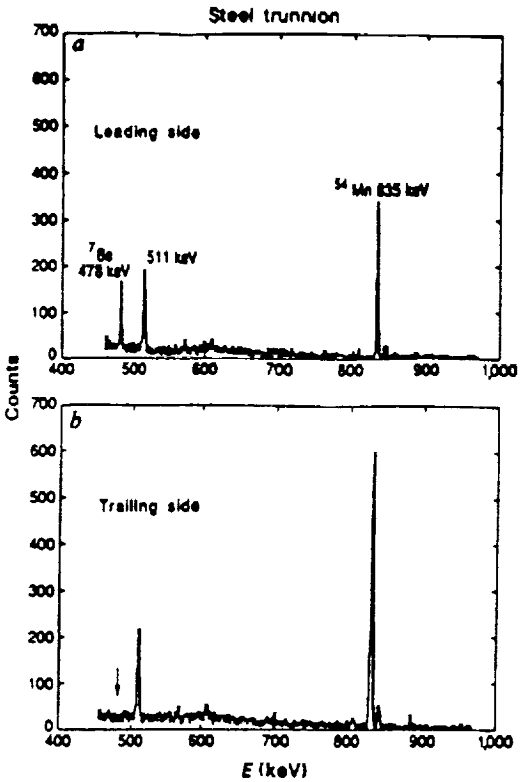

FIG. 3 Gamma-ray spectra of two stainless steel trunnion pin-end pieces from the leading and trailing directions of the spacecraft. As in Fig. 2, the ^{7}Be isotope is seen only on the leading side of LDEF. The 835-keV line from the spallation product ^{54}Mn is observed on both sides of the spacecraft, but is stronger on the trailing side due to increased proton flux from the west. Both spectra represent 12-h counts.

LDEF materials have not revealed other nuclides with similar surface segregation behaviour; in particular, we have not found the heavier ones that would suggest a meteoritic origin[17]. Whereas ^{7}Be will decay in orbit, there are other non-radioactive light isotopes produced by cosmic rays with similar altitude distributions. Their concentrations should be much higher than that of ^{7}Be, although more difficult to measure. We are currently attempting to detect other atmospheric cosmic-ray-produced isotopes on LDEF surfaces, such as ^{14}C and ^{10}Be, using accelerator mass spectrometry (A. J. T. Jull, personal communication).

The use of satellite surfaces to sweep up rare atmospheric species may prove to be a new method of investigating atmospheric mixing processes at orbital altitudes. □

Received 18 July 1990; accepted 4 January 1991.

1. Gregory, J. C. & Peters, P. N. in LDEF - The Long Duration Exposure Facility NASA SP-473 (eds Clark, L. et al.) 14 (NASA, Washington, DC, 1984).
2. Watts, J. W., Parnell, T. A. & Heckman, H. H. AIP Conf. Proc. 186—High Energy Radiation in Space (eds Rester, A. C. & Trombka, J. I.) 75 (AIP, New York, 1989).
3. Arnold, J. R. & Al-Salih, H. Science 121, 451 (1955).
4. Benioff, P. A. Phys. Rev. 104, 1122–1130 (1956).
5. Lal, D., Malhotra, P. K. & Peters, B. J. atmos. terr. Phys. 12, 306–328 (1958).
6. Lal, D. & Peters, B. Encyclopedia of Physics (ed. Sitte, K.) 46/2, 551–612 (Springer, New York, 1967).
7. Bhandari, N. J. geophys. Res. 75, 2927–2930 (1970).
8. O'Brien, K. J. geophys. Res. 84, 423–431 (1979).
9. Shapiro, M. H. & Forbes-Resha, J. L. J. geophys. Res. 81, 2647–2649 (1976).
10. Husain, L., Coffey, P. E., Meyers, R. E. & Cederwall, R. T. Geophys. Res. Lett. 4, 363–365 (1977).
11. Blechrodt, J. F. J. geophys. Res. 83, 3058–3062 (1978).
12. Viezee, W. & Singh, H. B. Geophys. Res. Lett. 7, 805–808 (1980).
13. Raisbeck, G. M. et al. Geophys. Res. Lett. 8, 1015–1018 (1981).
14. Sanak, J., Lambert, G. & Ardouin, B. Tellus 37B, 109–115 (1985).

Letters to Nature

15. Dutkiewicz, V. A. & Husain, L. J. geophys. Res. 90, 5783–5788 (1985).
16. Ellis, J. E. J. geophys. Res. 94, 2261–2286 (1989).
17. [illegible], P. A., [illegible], M. A., [illegible], P. & [illegible], J. Planet. Space Sci. 25, 1821–1842 (1977).

ACKNOWLEDGEMENTS. We are grateful for the outstanding support of the LDEF Project Office, NASA Langley Research Center and in particular, the LDEF Project Scientist, W. Kinard.

Low surface resistance in $YBa_2Cu_3O_x$ melt-processed thick films

N. McN. Alford*, T. W. Button*, M. J. Adams†, S. Hedges†, B. Nicholson† & W. A. Phillips‡

* ICI Advanced Materials, PO Box 11, The Heath, Runcorn, Cheshire WA7 4QE, UK
† GEC–Marconi Research, Great Baddow, Chelmsford, Essex CM2 8HN, UK
‡ GEC Hirst Research Centre, East Lane, Wembley, Middlesex HA9 7PP, UK

A LOW surface resistance, R_s, is the key to successful development of radio-frequency and microwave applications of high-temperature superconductors. Here we report the R_s of $YBa_2Cu_3O_x$ thick films on yttria-stabilized zirconia substrates at frequencies up to 50 GHz. Films processed below the peritectic temperature are fine grained, have R_s similar to bulk $YBa_2Cu_3O_x$, generally have low critical current density (J_c) and exhibit little preferred orientation of crystallographic axes. Films processed above the peritectic temperature exhibit preferred orientation in large spherulitic grains, have higher J_c and far lower R_s. For these films the crossover frequency at which R_s equals that of copper is 50 GHz, a factor of two higher than the best bulk material or thick film yet reported and only a factor of ~4 lower than high-quality thin films. At the frequencies used for mobile communications (900 MHz and 1.8 GHz), the superconductor losses would be two orders of magnitude lower than those of normal metals. The particular advantages of the thick-film route are the speed and low cost of the process, and the ability to apply the films on curved surfaces and on large areas, the largest so far being >200 cm^2.

Because the of the quadratic frequency dependence of R_s in superconductors[1], as opposed to the square-root dependence in normal metals, there is a great incentive to reduce R_s in superconductors so that operation of devices below the cross-over frequency benefit from a lower R_s than that of a normal metal. Measurements of R_s so far can be divided into two broad groups: those made on bulk[2] or thick-film samples prepared from powder and those on thin films prepared by sputtering, laser ablation or co-evaporation. The thin films, which are usually grown epitaxially with the c axis normal to the plane of the substrate, show losses that are typically lower by two orders of magnitude relative to bulk materials[2]. It is believed that the increased losses in bulk material arise from the weak links between the random array of crystallites which also reduce critical currents[3].

Our work was motivated by the need to provide an inexpensive, rapid and effective alternative to thin films for certain applications, and which can be used when thin-film methods are not possible for reasons of size or curvature. The thick-film process also has inherent advantages in that polycrystalline substrates of large size (~300 mm square) are readily available. The best thick films so far have been formed on silver substrates by electrophoretic deposition[4–6], and have an R_s at 21.5 GHz of 18±3 mΩ at 77 K. In that work, however, problems arose because of thermal mismatch with the substrate, causing spalling of the films; also, because silver was used as the substrate, the maximum processing temperature could not exceed ~930 °C. Our technique avoids these problems and gives extremely adherent films which have the lowest R_s for thick films yet reported.

The substrates used were comprised of polycrystalline 3 mol%